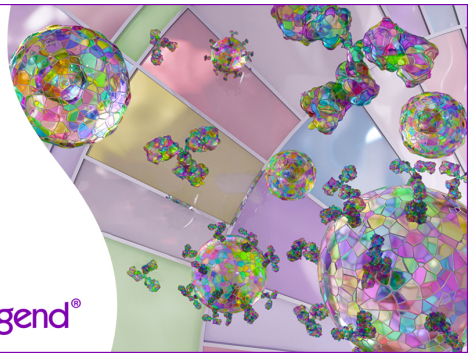

The Journal of Immunology
RESEARCH ARTICLE | DECEMBER 15 2010

The Inflammatory Response after an Epidermal Burn Depends on the Activities of Mouse Mast Cell Proteases 4 and 5 FREE

George Younan; ... et. al

J Immunol (2010) 185 (12): 7681–7690.
https://doi.org/10.4049/jimmunol.1002803

The Inflammatory Response after an Epidermal Burn Depends on the Activities of Mouse Mast Cell Proteases 4 and 5

George Younan,*,†,[1] Freeman Suber,*,†,[1] Wei Xing,†,‡,[1] Tong Shi,†,‡ Yuichi Kunori,§ Magnus Åbrink,¶ Gunnar Pejler,‖ Susan M. Schlenner,** Hans-Reimer Rodewald,** Francis D. Moore, Jr.,*,† Richard L. Stevens,†,‡ Roberto Adachi,†† K. Frank Austen,†,‡ and Michael F. Gurish†,‡

A second-degree epidermal scald burn in mice elicits an inflammatory response mediated by natural IgM directed to nonmuscle myosin with complement activation that results in ulceration and scarring. We find that such burn injury is associated with early mast cell (MC) degranulation and is absent in WBB6F1-*Kit*^{W}/*Kit*^{Wv} mice, which lack MCs in a context of other defects due to a mutation of the Kit receptor. To address further an MC role, we used transgenic strains with normal lineage development and a deficiency in a specific secretory granule component. Mouse strains lacking the MC-restricted chymase, mouse MC protease (mMCP)-4, or elastase, mMCP-5, show decreased injury after a second-degree scald burn, whereas mice lacking the MC-restricted tryptases, mMCP-6 and mMCP-7, or MC-specific carboxypeptidase A3 activity are not protected. Histologic sections showed some disruption of the epidermis at the scald site in the protected strains suggesting the possibility of topical reconstitution of full injury. Topical application of recombinant mMCP-5 or human neutrophil elastase to the scalded area increases epidermal injury with subsequent ulceration and scarring, both clinically and morphologically, in mMCP-5–deficient mice. Restoration of injury requires that topical administration of recombinant mMCP-5 occurs within the first hour postburn. Importantly, topical application of human MC chymase restores burn injury to scalded mMCP-4–deficient mice but not to mMCP-5–deficient mice revealing nonredundant actions for these two MC proteases in a model of innate inflammatory injury with remodeling. ***The Journal of Immunology*****, 2010, 185: 7681–7690.**

A superficial second-degree epidermal burn results in an initial cellular injury that is amplified by an acute inflammatory response that includes edema and an influx of neutrophils (1, 2). This inflammatory response is dependent on a natural IgM to uncovered epitopes and complement activation, which are also components in the process of ischemia–reperfusion (IR) injury of the mouse hind limb skeletal muscle (3–6). In IR injury of mouse hind limb skeletal muscle, we observed that myocyte injury occurred with reperfusion and was accompanied by progressive degranulation of mast cells (MCs) (7). The myocyte injury was known to be diminished in MC-deficient WBB6F1-*Kit*^{W}/*Kit*^{Wv} (WWv) mice (8, 9), and we observed significant protection in mice with targeted disruption of the elastase mouse MC protease (mMCP)-5 (7). There was no protection against hind limb IR injury in strains lacking the MC-specific tryptase mMCP-7 or heparin proteoglycan or other proinflammatory functions such as generation of TNF-α, expression of transmembrane tryptase (Prss31), and generation of the eicosanoids, prostaglandin D_2 or the leukotriene C_4 (7).

MCs are highly specialized innate immune effector cells that contain secretory granules in which large amounts of proteases are stored in complexes with serglycin proteoglycans (reviewed in Refs. 10, 11). These proteases represent at least three classes of protease activities in mice (12–14) and in humans (15–17), chymotrypsin-like (chymases), trypsin-like (tryptases), and a carboxypeptidase A (CPA3). Rat and mouse skin MCs also contain a unique protease, rMCP-5 and mMCP-5, respectively, which is highly homologous to the chymases and encoded by a gene in the chymase locus on mouse chromosome 14 (18, 19). However, unlike the mouse MC chymases, such as mMCP-1 in mucosal MCs and mMCP-4 in skin and connective tissue MCs, rat and mouse MCP-5 have an elastase-like specificity due to the presence of a valine instead of a glycine at position 216 (20–22). Studies with transgenic mice that lack MC-restricted serine proteases have revealed that some of these enzymes have prominent roles in innate immunity and inflammation. For example, mMCP-1–deficient mice have diminished ability to reject adult *Trichinella spiralis* nematodes from

*Department of Surgery and ‡Division of Rheumatology, Immunology, and Allergy, Department of Medicine, Brigham and Women's Hospital; †Harvard Medical School, Boston, MA 02115; §Biologics Discovery Research Group, Exploratory Technology Laboratories, Teijin Institute for Bio-medical Research, Teijin Pharma Limited, Tokyo, Japan; ¶Department of Medical Biochemistry and Microbiology, Uppsala University; ‖Department of Anatomy, Physiology and Biochemistry, Swedish University of Agricultural Sciences, Uppsala, Sweden; **Institute for Immunology, University of Ulm, Ulm, Germany; and ††Department of Pulmonary Medicine, The University of Texas M. D. Anderson Cancer Center, Houston, TX 77030

[1]G.Y., F.S., and W.X. contributed equally to this work.

Received for publication August 17, 2010. Accepted for publication October 12, 2010.

This work was supported by National Institutes of Health Grants GM 052585 and HL36110 and by Grants from the Swedish Medical Research Council, the Goran Gustafsson Foundation, and by the Deutsche Forschungsgemeinschaft (DFG RO-754/2-3). R.A. was supported by The University of Texas M. D. Anderson Cancer Center Physician Scientist Program.

Address correspondence and reprint request to Michael F. Gurish, Department of Medicine, Smith Research Building, Room 616, Brigham and Women's Hospital, 1 Jimmy Fund Way, Boston, MA 02115. E-mail address: mgurish@rics.bwh.harvard.edu

The online version of this article contains supplemental material.

Abbreviations used in this paper: CAE, chloroacetate esterase; chym, chymase; CPA3, carboxypeptidase A3; elast, elastase; HPF, high-power field; IR, ischemia–reperfusion; MC, mast cell; mMCP, mouse MC protease; NB, no burn; rmMCP-5, recombinant mMCP-5; WT, wild-type; WWv, WBB6F$_1$-*Kit*^{W}/*Kit*^{Wv}.

the small intestine (23), and mMCP-6–deficient mice have a reduced capacity to clear peritoneal infection by *Klebsiella pneumoniae* (24) and to recruit eosinophils to the site of *T. spiralis* larval encystment (25). These mMCP-6–deficient mice are also protected in models of inflammatory arthritis mediated by immune complexes (26, 27). CPA3 mutants with a functionally defective enzyme are unable to inactivate endothelin-1 or the homologous peptide from snake venom, sarafotoxin 6b (28).

Using a mouse model of an epidermal scald that results in a second-degree burn and that depends on natural IgM and serum complement (6), we found that the evolution of the wound from erythema to ulceration to scarring with loss of hair regrowth was prevented in the MC-deficient WWv strain. Significant protection against the progression of burn injury in skin after a scald was observed in mice with targeted disruption of mMCP-4 (chymase) or mMCP-5 (elastase), but not in mice lacking mMCP-6 and -7 (tryptases) or an enzymatically inactive form of CPA3. We then found that application of human MC chymase to the scald site of the mMCP-4–deficient strain and of recombinant mMCP-5 (rmMCP-5) or human neutrophil elastase, but not human chymase, to the scald site of the mMCP-5–deficient strain increased epithelial disruption and restored full burn injury with ulceration and scarring. Furthermore, MC degranulation to release the endogenous proteases occurred in the initial 2 h postscald burn. These findings extend the trauma-related functions of natural IgM, complement, and MCs to second-degree burns with progression to tissue remodeling; a result that may have implications for therapy in thermal injury and for other models of trauma-initiated inflammation-driven tissue pathology.

Materials and Methods

Animals

C57BL/6 mice were obtained from Taconic Laboratories (Germantown, NY) or The Jackson Laboratory (Bar Harbor, ME). MC-sufficient WBB6F1/J-*Kit*$^{+/+}$ and MC-deficient WBB6F1/J-*Kit*^{W}/*Kit*^{Wv}/J mice were obtained from The Jackson Laboratory. The mice deficient in mMCP-4 (N7), mMCP-5 (N10), and both mMCP-6 and mMCP-7 (N8) and those with an inactivating mutation of CPA3 (Mc-cpa^{Y356A,E378A} or Cpa3^{tmHrr}, N4) were on a C57BL/6 mouse genetic background, whereas the mice deficient in mMCP-1 were on a BALB/c background (7, 23, 24, 28–30). These protease-deficient strains were maintained in specific pathogen-free colonies at the Dana Farber Institute (Boston, MA) or in a barrier facility at Taconic Laboratories. Institutional animal care and use committee approval was obtained for all animal experiments, and the studies were conducted in accordance with the National Institutes of Health and Public Health Service guidelines for animal care.

Reagents

Human neutrophil elastase and human MC chymase were obtained from EMD Biosciences (La Jolla, CA) and Enzo Life Sciences International (Plymouth Meeting, PA). The chymase substrate S-2586 (MeO-Suc-Arg-Pro-Tyr-pNA) and the tryptase substrate S-2288 (H-D-Ile-Pro-Arg-pNA) were obtained from Chromogenix (Milano, Italy). The elastase substrate Suc-Ala-Ala-Pro-Val-pNA (S-AAPV) and the CPA3 substrate M-2245 (*N*-[4-methoxyphenylazoformyl]-Phe-OH) were obtained from Bachem (Torrance, CA). Mouse Ig, human lung tryptase, and bovine pancreatic CPA were obtained from Sigma-Aldrich (St. Louis, MO). Mouse anti-TNP IgE (C38-2), FITC-conjugated rat anti-mouse IgE (R35-72), and rat anti-mouse CD16/CD32 (2.4G2) were obtained from BD Biosciences (San Jose, CA). Allophycocyanin-Cy7 conjugated rat anti-mouse Kit (2B8) was obtained from eBioscience (San Diego, CA). Rabbit anti-peptide IgG for each protease was prepared as previously described (31, 32).

Recombinant mMCP-5 protein was prepared as described previously (20). Briefly, the cDNAs encoding mMCP-5 were obtained from total RNA extracted from the hearts of male C57BL/6 mice (Charles River Labs, Yokohama, Japan) by RT-PCR. After confirmation of the sequences, the cDNA fragments were cloned by transfer vector pFASTbac1 (Invitrogen, Carlsbad, CA), and recombinant baculovirus were generated by the Bac-to-Bac system (Invitrogen). For expression of the recombinant protein, Tn5 cells were grown in an Erlenmeyer flask (500 ml) to a density of 10^6 cells/ml in Ex-Cell 405 medium (200 ml/flask; Sigma-Aldrich) supplemented with 50 IU/ml penicillin and 50 mg/ml streptomycin in a rotary shaker (75 rounds/min) and were infected with the recombinant baculovirus at a multiplicity of infection of 1.0. After culture for 3 d at 28°C, the culture medium was centrifuged, and the supernatant was collected as a recombinant protein source. The recombinant promMCP-5 was purified by a column of heparin-cellurofine gel (Seikagaku-kougyo, Tokyo, Japan) and a column of phenyl-Sepharose CL-4B (Amersham Biosciences, Tokyo, Japan). The promMCP-5 was activated by treatment with bovine cathepsin C (Sigma-Aldrich) at room temperature for 7 d, purified on a column of heparin-cellurofine gel, and dialyzed with excess amount of pyrogen-free PBS for more than 24 h at 4°C. This preparation was used as the source of the purified rmMCP-5 after determination of protein concentration.

Epidermal scald procedure

The epidermal scald procedure was performed as previously described (6). Interscapular hair was removed from 10-wk-old male mice, and the next day, the mice were anesthetized with an i.p. injection of ketamine (10 mg/kg) and xylazine (20 mg/kg). After full sedation, a burn template, created from a high-impact nonheat-conducting plastic container, was used to produce a square-shaped 1-cm^2 wound on the interscapular dorsum area (~2.5% of the body surface area). With the template held in position, the shaved skin was scalded in a circulating water bath. After an initial temperature titration, all further experimentation was done at 54°C. The duration of scalding was 25 s when no dressing was applied to the burn, and 35 s when a dressing was applied immediately after the scald to allow for topical application of a protease. Increasing the duration of the scald was necessary to obtain burn injury because the application of the dressing apparently had a cooling or protective effect. All mice were treated for pain twice daily with s.c./i.m. injections of buprenorphine (0.05 mg/kg) for the first day postburn. The wound area was demarcated by denuded and erythematous skin by day 3.

For topical application of the proteases, they were diluted in HBSS, and 100 μl of the resulting solution was injected into a dressing that was created over the scalded area. The dressing consisted of a 1-cm^2 piece of gauze, wrapped inside a Duoderm frame and covered by a Tegaderm dressing (Fisher Scientific, Pittsburgh, PA). The wet dressing was applied immediately postscald and stayed on the burned area for 1 h unless otherwise indicated.

Histology and quantitative assessment of injury

Skin was harvested from the prepared dorsal sites before the burn and at 2 h, 3 d, and 12 or 13 d postburn. The tissue was fixed in 4% paraformaldehyde in PBS for 18 h, changed to PBS, and kept at 4°C. Sections were stained by Masson's trichrome or Jones' stain (methenamine silver–periodic acid–Schiff stain) or for chloroacetate esterase (CAE) reactivity, which involves a hematoxylin counterstain as previously described (7).

At 2 h postburn, CAE was employed to highlight MCs and neutrophil infiltration. MCs were examined under high power and quantified in unit areas (1 U area = 1.2 × 0.9 mm = 1.08 mm^2). Nine unit areas of the burn wound on each mouse were evaluated for total MC numbers and used to calculate the mean value (per 9 U areas) for each individual animal. An MC was determined to be degranulating when three or more granules could be found outside of the cell when it was examined under high power (7). Jones' staining was performed to demonstrate edema, which is indicated by decreased intensity of the stain relative to unburned mice. Injured epithelial cells and hair follicles were identified by the cytoplasmic vacuolization observed after CAE

At d 3 postburn, Masson's trichrome stain was used to differentiate denatured collagen (red staining) from viable collagen (blue staining) in the dermis of the burn wound. Digital photographs of the burn wound were taken at ×10 magnification (low-power field), and the degree of burn injury was evaluated by Image J software (National Institutes of Health, Bethesda, MD) based on the staining. The area of the burn was determined by measuring the area of denatured collagen (expressed in square-micrometers). To measure the depth of the burn and degree of edema, the thickness of the injured dermis (indicated by the denatured collagen), the thickness of the viable collagen in the dermis beneath the wound, and the thickness of the hypodermis were measured at three different locations, at the middle, left edge, and right edge of the burn. Values are the average of the three measurements and are expressed in micrometers. Injured hair follicles seen on photographs presented in this article were identified by disruption of the normal morphology including epithelial tight junctions, presence of necrotic cells, and loss of connection with the skin surface. Values were expressed as the average number of injured hair follicles per 4 high-power fields (HPF; ×40 magnification). Neutrophils in the same burn

wound were quantitated by CAE reactivity and expressed as the total number per 4 HPF.

At day 12 postburn, Masson's trichrome or Jones' stain was used to demonstrate granulation tissue formation and a decrement of normal collagen in the burn wound. With Masson's trichrome stain, the thickened epidermis was purple, and the granulation tissue in dermis was white in contrast with the surrounding dark-blue–stained collagen in normal dermis. With Jones' stain, the epidermis and granulation tissue were pink, and collagen in dermis was black. CAE reactivity was used to show MCs and neutrophils.

Characterization of mMCP-4– and mMCP-5–deficient strains for dermal MC numbers and proteases

The baseline levels of MCs in the interscapular skin, dermis, and hypodermis together were 134 ± 12.8 in wild-type (WT) mice, 97.7 ± 4.9 in mMCP-4–deficient mice, and 72.2 ± 14.3 in mMCP-5–deficient mice per 9 U areas (mean ± SE; n = 11, 6, and 5, respectively). The distributions of MCs were similar in all strains with the dermis containing 58.3% in WT mice, 48.4% in mMCP-4–deficient mice, and 47.4% in mMCP-5–deficient mice, and the hypodermis containing 41.7% in WT mice, 51.6% in mMCP-4–deficient mice, and 52.6% in mMCP-5–deficient mice.

To evaluate protease levels in these strains, lysates were prepared from purified peritoneal MCs obtained from C57BL/6 mice and from the various protease-deficient mice. Mixed peritoneal cells were obtained by lavage with modified Tyrode's buffer (0.02% KCl, 0.1% $NaHCO_3$, 0.005% NaH_2PO_4, 0.8% NaCl, 0.1% D-glucose, and 0.1% gelatin) (21), and the $Kit^+/Fc\varepsilon RI^+$ MCs were isolated by flow cytometry. Briefly, FcγRs were blocked with anti-CD16/CD32 Abs (10 μg/ml) and mouse Ig (100 μg/ml) for 10 min before staining. The peritoneal lavage cells were incubated with IgE in HBSS/FBS (2% FBS) for 1 h, washed twice, and stained with FITC–anti-IgE and allophycocyanin-Cy7–anti-Kit by incubation for 1 h more. Cells were washed twice with HBSS/FBS and isolated by FACS (MoFlo; DakoCytomation, Fort Collins, CO) at the Dana Farber Cancer Institute flow cytometry facility. Cells were kept on ice throughout the procedure. Lysates of sorted cells were prepared by sonication, and debris was removed by centrifugation. Sonicates were adjusted to represent equal numbers of cells per milliliter.

Reactions to determine enzymatic activities were carried out in 96-well plates. Samples of cell lysates or the reference proteases were incubated with chromogenic substrates in a final volume of 200 μl reaction buffer (100 mM Tris-HCl, 150 mM NaCl, 0.05% Tween 20, and 0.1% BSA, pH 8.5) at 37°C for 24 h. Chymase activity was measured with substrate S-2586 at 0.5 mM, elastase with S-AAPV at 1 mM, tryptase with S-2288 at 0.5 mM, and CPA3 with M-2245 at 1 mM (20, 21, 33–35). Enzymatic activities were assessed by measuring the OD at 405 nm after a 24-h incubation and were expressed as the amount of protease based on standard curves prepared with purified human neutrophil elastase, human MC chymase, human MC tryptase, or bovine CPA, each in the presence of 50 μg/ml heparin.

The dermal MCs in C57BL/6 (WT) mice express the chymase mMCP-4, the elastase mMCP-5, the MC-specific carboxypeptidase CPA3, and the tryptase mMCP-6 but lack the tryptase mMCP-7 due to a mutation at the exon 2/intron 2 splice site (36, 37). The targeted deletion of CPA3 alters the expression of other proteases (38), whereas the CPA3 activity-deficient ($CPA3_{act}^{-/-}$) strain with nonfunctional CPA3 is similar to WT mice in the expression of the other proteases (28). As the integrity of the other proteases has not been fully assessed in mMCP-4–, mMCP-5–, and mMCP-6/7–targeted strains, we compared the level of chymase (mMCP-4), elastase (mMCP-5), tryptase (mMCP-6), and CPA3 enzymatic activities in purified peritoneal MCs from these strains with those in the MCs from WT mice. The peritoneal MCs isolated from mMCP-4–deficient mice had no detectable chymase activity, normal levels of elastase and CPA3 activities, and enhanced tryptase activity (387% of WT level) (Supplemental Fig. 1*A–D*). Peritoneal MCs isolated from mMCP-5–deficient mice had no elastase activity, markedly reduced chymase (10% of WT level) and CPA3 activities (<3% of WT level), but enhanced tryptase activity (421% of WT level). Peritoneal MCs isolated from mMCP-6/7–deficient mice had markedly reduced tryptase activity (14% of WT level) and normal levels of elastase, chymase, and CPA3. The residual tryptic activity is presumably due to the presence of transmembrane tryptase/tryptase γ/Prss31 in these cells. The reduced expression of mMCP-4 in mMCP-5–deficient mice was confirmed by immunoblot analysis using peritoneal MC lysates (Supplemental Fig. 1*E*)

Statistical analysis

Student t test for unpaired samples was used for direct comparisons of means of observations made in various animals. A p value <0.05 was considered significant.

Results

Epidermal scald injury is MC-dependent at 54°C

In an initial clinical screen to evaluate whether we could identify an intensity of scald burn injury that required mature cutaneous MCs for development of an ulcer and subsequent remodeling, we compared the injury generated in MC-sufficient WBB6F1/J mice versus that in MC-deficient WWv littermates by exposing a 1-cm^2 area of dorsal epidermis to water heated to 54°C, 56°C, or 58°C for 25 s. The WWv strain of mice have <1% of the normal number of skin MCs (39). All of the MC-sufficient mice exhibited burn injury by day 3 postscald with erythema and ulceration at each temperature (Fig. 1). Over the next 10 d, the ulcerated skin healed with scarring and loss of hair regrowth. In contrast, after a 54°C scald, the MC-deficient WWv mice showed little or no erythema and no ulceration on day 3 with full reappearance of hair on day 13. However, after a scald burn at 56°C or 58°C, the ulceration at day 3 and scarring without hair regrowth at day l3 in the MC-deficient mice was similar to that observed in the MC-sufficient controls indicating a MC-independent injury process at these higher temperatures.

Histological characterization of the scald burn

We characterized the histologic changes of a 54°C scald burn compared with the histologic condition of unburned sites in C57BL/6 (WT) mice 2 h, 3 d, and 12 d postscald. At 2 h postburn, the epidermis showed cytoplasmic vacuolization and disruption of the tight junctions between the basal cells of the epithelium (Fig. 2*A*, black arrow). The involved hair follicles showed mild hydropic swelling and disruption of the epithelium of the follicles (Fig. 2*A*, red arrow). Many of the MCs in the dermis (Fig. 2*B*, arrows) and hypodermis (Fig. 2*C*, black arrows) were degranulating after the burn (48.6 ± 14.3% and 61.1 ± 14.9%, respectively, mean ± SE; n = 5 from three separate experiments). In the hypodermis, there was vasodilatation, vascular stasis, vascular thrombosis, marginated neutrophils within the blood vessels (red arrow), and an influx of neutrophils into the tissue at 2 h postburn (Fig. 2*C*). In both the

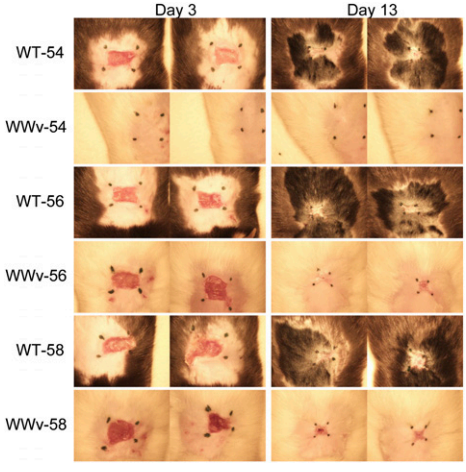

FIGURE 1. MC-deficient mice are protected against epidermal scald injury at 54°C. The clinical response to an epidermal scald of 25-s duration in MC-sufficient WBB6F1 (WT) mice and MC-deficient WWv mice was compared at three different temperatures at 3 and 13 d after injury. Photographs show the two mice in each group. Hair regrowth at the scald site of the 54°C-treated WWv mice is not seen due to its lack of pigment. The black marks were replaced each day to define the residual injury and do not represent the area of the original scald site. Protection against a visible burn in MC-deficient mice exposed to a 54°C scald for 25 s was confirmed in two further experiments with sufficient and deficient strains with five mice per group.

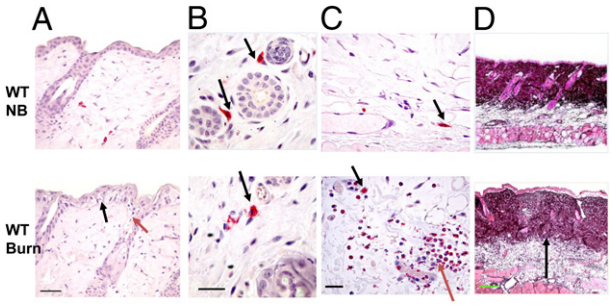

FIGURE 2. Histological changes occurring 2 h after a scald burn in the skin of WT C57BL/6 mice. The histologic changes in the shaved skin in WT mice without (*top panels*) and with a scald burn of 25-s duration at 54°C (*bottom panels*) are compared at 2 h postburn. Sections in *A–C* are stained for CAE reactivity. *A*, Epidermis at the burn site shows disruption of the tight junctions between the basal cells of the epithelium (black arrow) and cytoplasmic vacuolization in epithelial cells of the epidermis and the hair follicles (red arrow). *B*, MCs in the dermis at the shaved site are intact (arrows, *top panel*), whereas MCs are degranulating with extracellular granules 2 h after the scald burn (arrow, *bottom panel*). *C*, Similarly, MCs in the hypodermis at the shaved site are intact (arrow, *top panel*) whereas 2 h after the scald burn they are degranulating (black arrow, *bottom panel*). There is also neutrophil margination in a blood vessel and influx into the hypodermis (red arrow). *D*, Jones' stain shows lighter staining of the collagen matrix of the dermis and expansion of the hypodermis at the scald site due to edema (arrow in *bottom panel* denotes depth of hypodermis). Scale bars and original magnifications: *A*, 50 μm, ×40; *B* and *C*, 25 μm, ×63; *D*, 200 μm, ×10. NB, no burn.

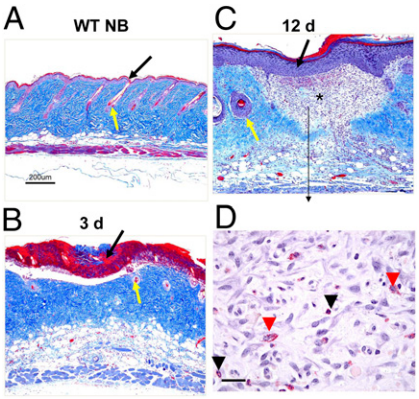

FIGURE 3. Histologic changes occurring at 3 d and 12 d after a scald burn in WT mice. *A–C* are stained with Masson's trichrome, and *D* is stained for CAE reactivity. *A*, WT mice with no burn show intact epithelium (black arrow) and hair follicles (yellow arrow). *B*, The epidermis 3 d postburn is denuded leaving an ulceration demarcated by denatured collagen (stained red, black arrow). The denatured collagen extends through about one half the dermis reflecting the breadth and depth of the burn and loss of hair follicles (yellow arrow). *C*, By 12 d postburn, the morphological changes include a thickened epithelium covering the wound (black arrow), granulation tissue without any hair follicles in the dermis (star), and damaged hair follicles at the edge of the scar (yellow arrow). *D*, High-power photograph of the granulation tissue shows accumulation of fibroblasts, MCs (red arrowhead), and neutrophils (black arrowhead). Scale bars and original magnifications: *A–C*, 200 μm, ×10; *D*, 25 μm, ×40. NB, no burn.

dermis and hypodermis, there was edema. This is apparent in the dermis by the separation of collagen fibers with lighter coloration of the dark-stained collagen and in the hypodermis by expansion of the tissue (Fig. 2*D*, arrow).

At 3 d postburn, coagulative necrosis at the burn site affected the entire thickness of the epidermis and about half the depth of the dermis (Fig. 3*B*). The epidermis was denuded, leaving an ulceration demarcated by denatured collagen (Fig. 3*B*, stained red; black arrow). Hair follicles in the dermis were destroyed (Fig. 3*B*, yellow arrow). The red-staining denatured collagen in the dermis was surrounded by a rim of capillary stasis and neutrophil infiltration. The inflammation in the hypodermis was sustained with vasodilatation and scattered neutrophil infiltration.

By 12 d postburn, the morphological changes included a thickened epithelium covering the wound (Fig. 3*C*, black arrow), no hair follicle regrowth in the dermis with damaged hair follicles at the edge of the scar (Fig. 3*C*, yellow arrow) and areas of granulation tissue (Fig. 3*C* [star], 3*D*). The granulation tissue contained numerous fibroblasts, MCs, and neutrophils (Fig. 3*D*). We evaluated changes in the area of the exposed skin over this time period in other studies by marking the initial burn site corners with a permanent tattoo and noted no contracture of the wound area (data not shown).

Mice deficient in mMCP-4 and mMCP-5 are protected from epidermal scald injury

In contrast with the clinical presentation of a scald burn with erythema and ulceration in WT C57BL/6 mice, mice lacking the chymase mMCP-4 or the elastase mMCP-5 showed little erythema and no ulceration at 3 d postscald burn (Fig. 4*A*). Mice lacking the tryptases, mMCP-6/7, or the carboxypeptidase CPA3 activity responded to the scald burn like the WT mice with erythema and ulceration. By histology, the scald burn site in mMCP-4$^{-/-}$ or mMCP-5$^{-/-}$ mice in this experiment showed little of the disruption of the epithelium, denaturation of collagen, loss of hair follicles, and edema of the dermis seen in WT as well as in mMCP-6/7– or CPA3$_{act}$-deficient mice (Fig. 4*B*). The mean histologically determined burn area in 20 WT mice pooled from three separate experiments was used to establish the normal range of injury ($154.2 \pm 23.3 \times 10^3$ μm^2), and this was compared with the injury observed in the various protease-deficient strains from one experiment each. The results revealed significant protection in mice lacking mMCP-4 or mMCP-5 (mean area ± SE, $3.1 \pm 2.2 \times 10^3$ and $15.6 \pm 11.1 \times 10^3$ μm^2 with $p < 0.001$ for both; $n = 4$ for both strains), whereas there was injury similar to WT mice in the mice lacking mMCP-6/7 or CPA3$_{act}$ ($90.9 \pm 44.0 \times 10^3$ and $109.9 \pm 34.9 \times 10^3$ μm^2; $n = 6$ and 5, respectively) (Fig. 4*C*). The aggregate studies at day 3 did show some clinical injury, erythema with ulceration, in 3 of 9 mMCP-4–deficient and 5 of 17 mMCP-5–deficient mice from 3 independent experiments, whereas the injury was similar to that of WT mice in 9 of 12 mMCP-6/7$^{-/-}$ mice (2 experiments) and 4 of 5 mice with the inactivating mutation in CPA3 (1 experiment). Furthermore, 2 of 2 mice lacking the mucosal MC chymase mMCP-1, which is not expressed in skin MCs, also exhibited full burn injury with ulceration and scarring (data not shown).

The protection against a scald burn in the mMCP-4– and mMCP-5–deficient strains prompted a further histological assessment for epidermal injury at 2 h under a higher-power view. Whereas there were rare to no vacuoles in the shaved unburned epidermal skin, there was extensive vacuolization of the epidermal cells and disruption of the tight junctions at the scald site 2 h postburn in WT mice. In the scald site of the mMCP-4$^{-/-}$ and mMCP-5$^{-/-}$ strains, the vacuoles were few and the disruption of the tight junctions was much less than in the WT mice (Fig. 4*D*). In the mMCP-4$^{-/-}$ mice, the percentage of MCs undergoing degranulation at 2 h postburn was 24.8 ± 8.0% and 34.2 ± 6.4% in the dermis and hypodermis, respectively (mean ± SE, $n = 4$ mice), which is about half of that observed in WT mice, although the differences are not significant given the limited sample size of four to five mice. Degranulation also was present in the scalded mMCP-5–deficient mice, but the weak staining of granules due to the low level of the

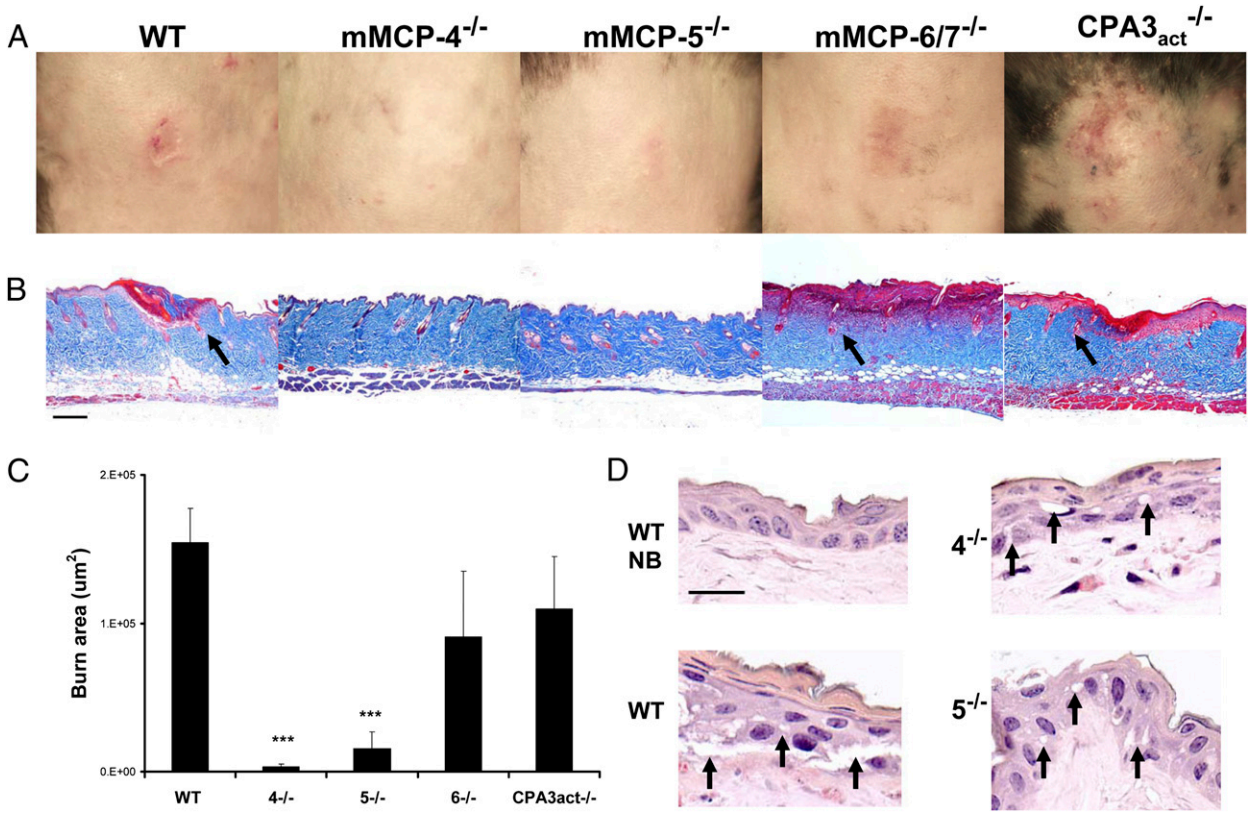

FIGURE 4. Absence of MC-specific secretory granule proteases, mMCP-4 or mMCP-5, protects against epidermal scald injury. *A*, The progression of clinical injury to ulceration at day 3 occurs in the WT, mMCP-6/7–deficient, and $CPA3_{act}$-deficient mice, but not in mMCP-4– or mMCP-5–deficient mice. *B*, The corresponding histological sections after Masson's trichrome staining to assess the breadth and depth of injury by the appearance of denatured collagen (red), injured hair follicles (arrows), and edema of the dermis revealed by thickness and lighter staining. Each picture is from a single mouse representative of the injury characteristic of each strain. *C*, Burn injury area (red area of denatured collagen in histological sections) in the same groups as in *A*. Values for the burn area are the mean (±SE) square-micrometers (1E+05 = 100,000). The value for the WT mice is derived from 3 experiments with 20 mice, and the other values are from 1 experiment with 4, 4, 6, and 5 mice, respectively. Statistical values are from a *t* test relative to the WT value. *D*, A high magnification of the epidermis in unburned WT (NB) and in burned WT, mMCP-$4^{-/-}$ ($4^{-/-}$), and mMCP-$5^{-/-}$ ($5^{-/-}$) mice at 2 h postburn shows disruption of epithelial tight junctions and epithelial vacuolization (arrows) in the burned WT mice but only minimal changes in these parameters mMCP-$4^{-/-}$ and mMCP-$5^{-/-}$ strains. Additional histologic data showing protection in the mMCP-4– and mMCP-5–deficient strains are shown in Fig. 5 and quantitated in Fig. 6. Scale bars and original magnifications: *B*, 200 μm, ×10; *D*, 20 μm, ×63. NB, not burned. ***$p < 0.001$.

associated proteases prevented reliable quantitation of intact cells and released granules. Thus, these studies implicated the connective tissue type MC and its secretory granule chymase, mMCP-4, and elastase, mMCP-5, but not its tryptases or MC-specific CPA3 in the early events leading to the ulceration and further suggested that these two proteases could play a role in the early epidermal changes.

Topical application of rmMCP-5 or human elastase to the burn site of mMCP-$5^{-/-}$ mice and of human MC chymase to the burn site of mMCP-$4^{-/-}$ mice reconstitutes scald burn injury

To support the findings that two different secretory granule proteases of mouse skin MCs were essential to the ulceration and scarring in our scald burn model, we sought to reconstitute injury by topical application of human chymase to mMCP-$4^{-/-}$ mice and of rmMCP-5 or human neutrophil elastase (elastase) to mMCP-$5^{-/-}$ mice. Each protease was applied to the scald burn site immediately after the burn, and the dressing was left in place for a period of 1 h. Control mice received a dressing with an equal volume of HBSS. This route of administration seemed reasonable not only because of the known loss of the skin permeability barrier function caused by a scald burn (6) but also because of our histologic finding of minimal but distinct disruption of the epidermis in the protected protease-deficient mice (Fig. 4*D*). The mMCP-$4^{-/-}$ mice received a total dose of 10 μg human chymase, and the mMCP-$5^{-/-}$ mice received either a total dose of 1 μg rmMCP-5 or 10 μg human elastase. At day 3 postburn, the scald site in the mMCP-4– and mMCP-5–deficient strains treated with HBSS was without ulceration or significant edema, whereas the chymase-treated site in the mMCP-$4^{-/-}$ mice and the rmMCP-5– or elastase-treated sites in the mMCP-$5^{-/-}$ mice showed significant injury on histologic analysis with coagulation necrosis of the epidermis, loss of hair follicles, and denaturation of collagen and edema in the dermis (Fig. 5).

To quantify the changes at day 3 elicited by application of the missing protease activity to the burn site, we compared the mean burn area, neutrophil influx in the hypodermis, number of injured hair follicles, and thickness of the skin in these various groups. To establish the range of injury in the HBSS-treated WT mice for comparison with the various protease-deficient strains treated with various reagents, we evaluated these values in 16 WT mice from 3 independent experiments with the reconstitution protocol. The mean burn area of HBSS-treated WT mice was $133.8 \pm 26.4 \times 10^3$ μm^2 (Fig. 6*A*), similar to that observed in the nontreated WT mice (Fig. 4*C*). In contrast, the mean burn area of the HBSS-treated mMCP-4– and mMCP-5–deficient strains was significantly less (0 ± 0 and $4.7 \pm 1.4 \times 10^3$ μm^2, respectively, mean ± SE; $n = 4$ from 1 experiment and $n = 7$ from 2 experiments; $p < 0.001$ for

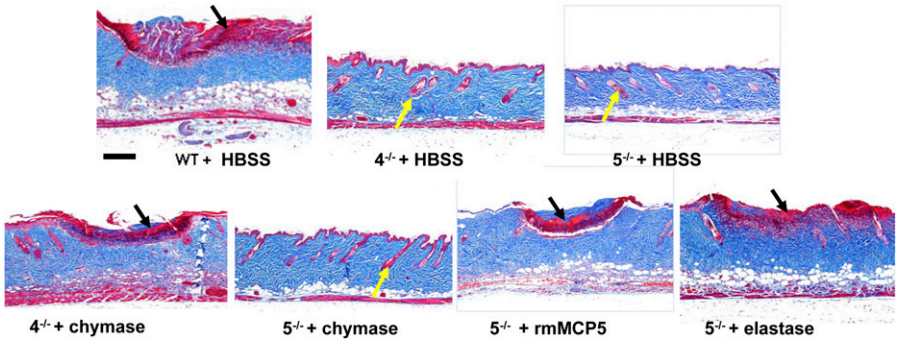

FIGURE 5. Topical application of human chymase and of recombinant mMCP-5 or human elastase reconstitutes the histologic changes of scald burn injury in mMCP-4$^{-/-}$ and mMCP-5$^{-/-}$ strains, respectively. WT, mMCP-4$^{-/-}$ (4$^{-/-}$), and mMCP-5$^{-/-}$ (5$^{-/-}$) mice were burned for 35 s at 54°C and treated topically with a dressing providing HBSS, human chymase (chymase), rmMCP-5, or human elastase (elastase) for 1 h postburn. Masson's trichrome staining of scald site is depicted at day 3. The injury is indicated by the red-staining denatured collagen (black arrows), and protection is indicated by absence of denatured collagen and the presence of intact hair follicles (yellow arrows). Sections are representative of the aggregate findings for each group presented in Fig. 6. Scale bar: 200 μm. Original magnification ×10.

both; Fig. 6*A*). The mean area of the burn in the mMCP-4$^{-/-}$ mice given topical human chymase (243.1 ± 25.1 × 10^3 μm^2) and in the mMCP-5$^{-/-}$ mice given topical rmMCP-5 (167.3 ± 53.1 × 10^3 μm^2) or human elastase (121.6 ± 32.0 × 10^3 μm^2) was significantly greater than that of their respective protease-deficient, HBSS-treated controls ($p < 0.001$, $p < 0.05$, and $p < 0.05$; $n = 5, 5, 4$, respectively; 1 experiment each) and similar to that of the WT mice (Fig. 6*A*). The mMCP-5$^{-/-}$ mice treated with chymase showed no significant increment in burn area (27.2 ± 22.5 × 10^3 μm^2; $n = 5$; 1 experiment) relative to the HBSS-treated mMCP-5–deficient mice.

The number of injured hair follicles in mMCP-4$^{-/-}$ and mMCP-5$^{-/-}$ mice treated with HBSS was negligible and significantly less than that in WT mice treated with HBSS ($p < 0.001$ for both). The

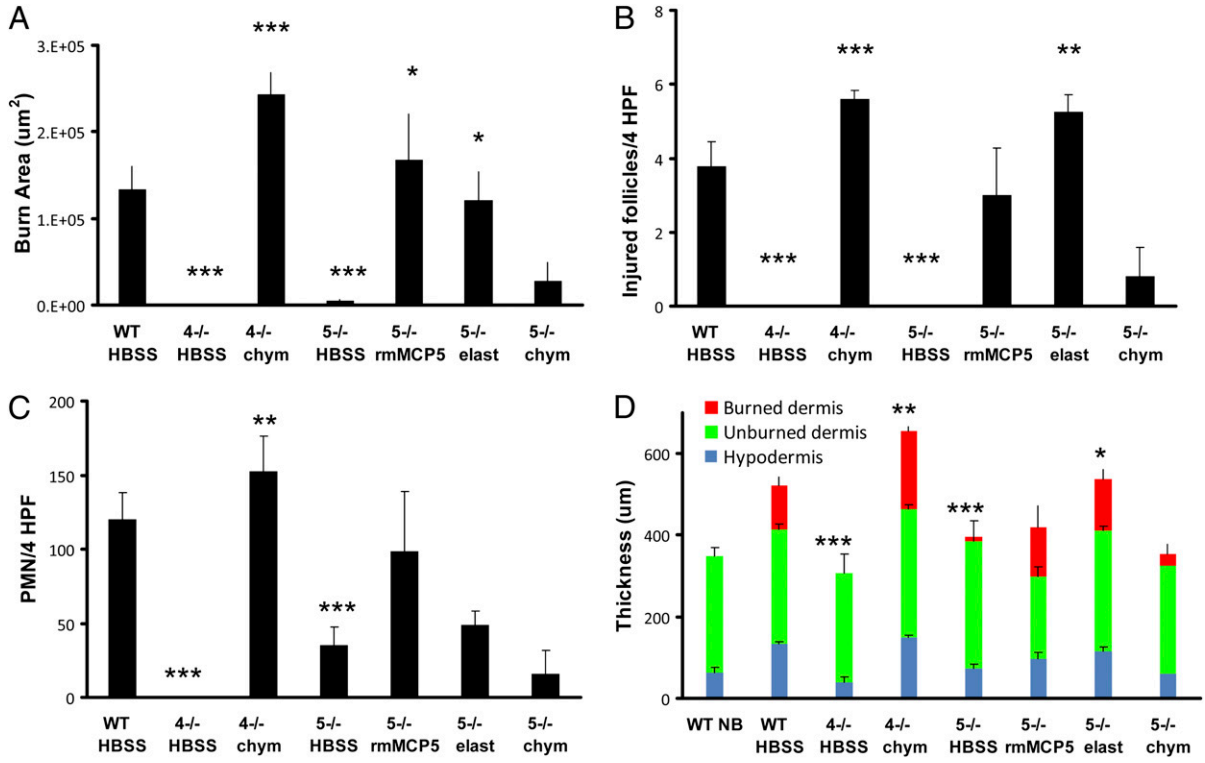

FIGURE 6. Quantitative assessment of burn injury after the topical application of human chymase to mMCP4$^{-/-}$ mice and of rmMCP-5 or human elastase to mMCP-5$^{-/-}$ mice. Mice were burned for 35 s at 54°C, then treated with topically applied HBSS, chymase, rmMCP-5, or elastase as indicated for 1 h and the injury evaluated on day 3 postscald burn. *A*, The mean area (±SE) of burn injury area was assessed by Masson's trichrome staining (1E+05 = 100,000). The value for the WT mice is derived from three experiments with 16 mice. The value for the HBSS-treated mMCP-5$^{-/-}$ is derived from two experiments, and all others are from one experiment. Numbers of mice are 16, 4, 5, 7, 5, 4, and 5 in each group, respectively. *B*, The mean number (±SE) of injured hair follicles (per 4 high-power field [HPF]) in the same animals as in *A*. *C*, The mean number (±SE) of neutrophils (per 4 HPF) identified by CAE reactivity in the hypodermis of the same animals as in *A*. *D*, The mean depth (±SE) of the skin from the same mice as in *A* with the depth of the various individual tissues indicated by burned dermis (red), unburned dermis (green), and hypodermis (blue). The mean (±½ range) values from two nonburned WT (WT NB) mice are shown for comparison. For statistical analysis, the mMCP-4– and mMCP-5–deficient mice treated with HBSS were compared with the WT controls, whereas the enzyme reconstituted groups were compared with the respective HBSS-treated strain. *A–D*: *$p < 0.05$; **$p < 0.01$; ***$p < 0.001$. chym, chymase; elast, elastase.

mMCP-4$^{-/-}$ mice treated with chymase or the mMCP-5$^{-/-}$ mice treated with human elastase had a significant increase in injured hair follicles compared with that in the same strain treated with HBSS ($p < 0.001$ and $p < 0.01$, respectively), whereas the response to rmMCP-5 did not reach significance ($p = 0.08$) (Fig. 6*B*). The mMCP-5$^{-/-}$ mice treated with chymase showed few injured follicles, similar to their HBSS-treated controls. By comparison with burned WT mice, the neutrophil influx into the hypodermis was significantly decreased in mMCP-4$^{-/-}$ and mMCP-5$^{-/-}$ mice ($p < 0.001$ for both). With topical application of chymase, the scald burn in mMCP-4$^{-/-}$ mice showed a significant increase in neutrophil influx into the hypodermis, whereas the increase in neutrophils in the burn of mMCP-5$^{-/-}$ mice treated with either rmMCP-5 or elastase did not reach significance (Fig. 6*C*). The thickness of the dermis and hypodermis (used as a marker of edema) was significantly less in the mMCP-4$^{-/-}$ and mMCP-5$^{-/-}$ mice given saline ($p < 0.001$ for both) compared with that in WT mice, and this was significantly increased by topical treatment of the appropriate deficient mice with chymase or elastase, respectively (Fig. 6*D*). A significant change in thickness was not observed in mMCP-5$^{-/-}$ mice given rmMCP-5 or chymase. Thus, the reconstitution of protease-deficient mice with the respective activity of the missing enzyme restored much of the histologic burn injury at 3 d.

To see if topical protease reconstitution had an effect at 2 h postburn, we compared the histology of the scald site in the deficient strains treated with enzyme or buffer. The minimal but definite disruption of the epidermal basal layer at the burn site in the mMCP-4– and mMCP-5–deficient mice was increased with topical protease treatment (Fig. 7*A*, arrows), resembling the cytoplasmic vacuolization and disruption of tight junctions seen in a scald injury of a WT strain at the same time point (Figs. 2*A* and 4*D*). Similarly, in these protease-deficient mice, the topical application of the missing protease function postscald resulted in increased vasodilation and edema in both dermis and hypodermis indicated by lighter staining of dermal collagen and increased hypodermal thickness (Fig. 7*B*), again resembling the response of the WT strain (Fig. 2*D*). There was increased neutrophil margination and influx into the hypodermis with chymase treatment of the mMCP-4$^{-/-}$ mice and with rmMCP-5$^{-/-}$ treatment of the mMCP-5$^{-/-}$ mice (Fig. 7*C*), which is compatible with their presence at this time point in scalded WT mice (Fig. 2*C*).

At d 12 postburn, none of the remodeling changes that occur in WT mice were observed in the protected mMCP-4– or mMCP-5–deficient mice, which had a normal epidermal layer and normal dermis with intact hair follicles and sebaceous glands (Fig. 8). In contrast, the scald site in mMCP-4–deficient mice treated with chymase and in the mMCP-5–deficient mice treated with rmMCP-5 showed the thickened epithelium, formation of granulation tissue (light-pink staining, yellow arrow) in the dermis, and loss of hair follicles comparable with that of the scalded WT mice (Fig. 3*C*)

We also evaluated the timing needed for topical application of rmMCP-5 to restore clinical burn injury in mMCP-5–deficient mice at day 3. We applied 400 ng of the recombinant enzyme for 1 h immediately after injury or after a delay of 1, 3, 6, or 24 h. Each of nine mMCP-5–deficient mice receiving rmMCP-5 immediately postburn or with a delay of 1 h exhibited erythema and ulceration comparable with that of the WT mice treated in parallel. However, when the topical application of rmMCP-5 was delayed to 3 h or more, 13 of 14 mMCP-5$^{-/-}$ mice exhibited protection from clinical injury. We also noted that 10 μg of topically applied elastase failed to reconstitute the clinical burn in the mMCP-4–deficient strain (data not shown).

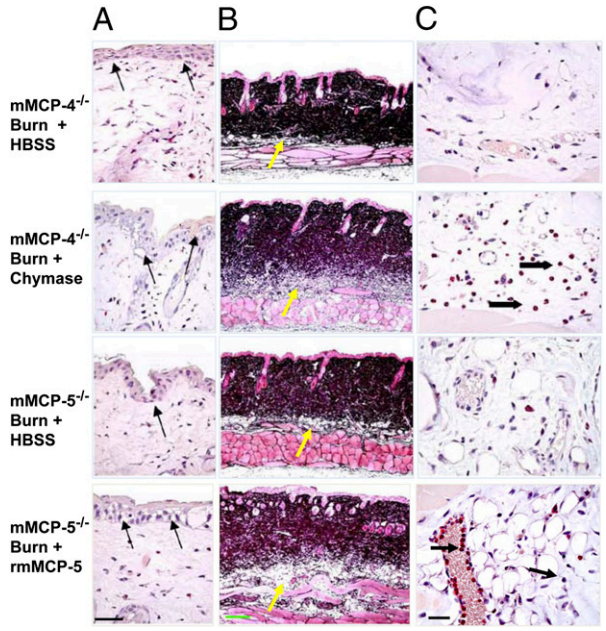

FIGURE 7. Histological changes 2 h after an epidermal scald in the skin of mMCP-4– and mMCP-5–deficient mice without and with topical application of human MC chymase or rmMCP-5, respectively. All mice were treated with topical HBSS with or without a protease for the first hour postburn. *A*, Cytoplasmic vacuolization and disruption of the tight junctions between the basal cells of the epithelium at the scald site is apparent after CAE staining in the protease-deficient strains and is accentuated with topical application of chymase to the mMCP-4–deficient strain and of rmMCP-5 to the mMCP-5–deficient strain (arrows). *B*, Jones' staining shows increased edema as indicated by the lighter color of the dermis and greater depth of the hypodermis (yellow arrows) in mMCP-4$^{-/-}$ mice treated with chymase and in mMCP-5$^{-/-}$ mice treated with rmMCP-5 relative to their HBBS-treated protease-deficient controls. *C*, The CAE reactivity in the hypodermis shows neutrophils (arrows) in the blood vessels and tissue of mMCP-4$^{-/-}$ mice treated with chymase and in mMCP-5$^{-/-}$ mice treated with rmMCP-5. Scale bars and original magnifications: *A*, 50 μm, ×63; *B*, 200 μm, ×10; *C*, 25 μm, ×63.

Discussion

The findings that two secretory granule serine proteases of cutaneous and connective tissue MCs, mMCP-4, a chymase, and mMCP-5, an elastase, are required for a scald injury to progress to a second-degree burn in the mice manifested by ulceration and subsequent scaring without hair regrowth extends the role of these proteases previously recognized as critical to IR injury in hind limb muscle (7). Both models also require natural IgM and activation of the complement pathway, implicating an innate autologous pathway to injury (3–6). The progressive histologic changes at the site of the scald burn in WT mice include disruption of the epidermal basal layer, degranulation of MCs and edema of the dermis and hypodermis at 2 h, denuding of the epidermis with wound erosion and destruction of the hair follicles by day 3, and remodeling with failure to regrow hair by 9–13 d.

The scald burn injury to the epidermis is evident as early as 2 h postburn by some vacuolization and disruption of the tight junctions between the epidermal cells at the scald site even in the protease-deficient strains, which failed to show progression of the injury to ulceration and remodeling. This suggested that there could be an early permeability change in the epidermis that might allow a topical approach to restore the protease-dependent component of the full response to burn injury in the protected mMCP-4– and mMCP-5–deficient strains. Indeed, the topical application immediately postscald of rmMCP-5 or human neutrophil elastase to

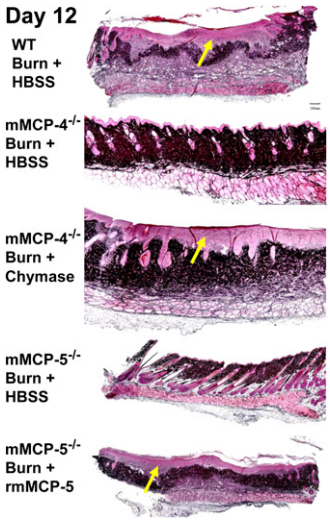

FIGURE 8. Topical application of chymase and rmMCP-5 to the burn site on mMCP-4$^{-/-}$ and mMCP-5$^{-/-}$ mice, respectively, leads to remodeling at day 12. Jones' stain of the skin reveals thickened epithelium, granulation tissue (light pink; yellow arrows), and loss of hair follicles in WT mice, in mMCP-4$^{-/-}$ mice treated with chymase, and in mMCP-5$^{-/-}$ mice treated with rmMCP-5, whereas the protease-deficient mice treated with HBSS alone had normal epithelium, hair follicles, and sebaceous glands. Scale bar: 200 μm. Original magnification ×10.

the mMCP-5–deficient mouse or of human MC chymase to the mMCP-4–deficient mouse increased the epidermal disruption and fully restored the downstream aspects of the burn injury. The resultant edema of dermis and hypodermis and influx of neutrophils at 2 h postburn, ulceration with collagen denaturation of the dermis and necrosis of the hair follicles at 3 d, and scar formation without hair regrowth at 9–13 d resembled the burn injury of WT mice. The requirement for the specificity of both proteases for scald burn progression is supported by the failure of chymase to restore clinical and histologic progression of injury in the mMCP-5–deficient strain and the failure of elastase to reconstitute the clinical injury in the mMCP-4–deficient strain. The aggregate data suggest that MC activation with nonredundant protease-dependent epidermal injury initiates or is an essential component of the processes leading to ulceration and remodeling of the burn site.

The availability of mouse strains deficient in different secretory granule proteases was critical to our study for two major reasons. First, these strains have none of the hematologic and cellular defects due to the mutation of *Kit* in the WWv strain. For the burn model, this difference could be important because neutrophil infiltration does occur early in the dermis and hypodermis of the burn site in WT mice, and the WWv stain is neutropenic and has impaired neutrophil mobilization to tissues (40, 41). Second, the range of mice with targeted deletion of MC-specific proteases and normal MC numbers allowed identification of the particular secretory granule proteases participating in the scald burn injury model.

Skin and connective tissue MCs of most mouse strains express the tryptases mMCP-6 and mMCP-7, the chymase mMCP-4, the elastase mMCP-5, and the exopeptidase CPA3, whereas the T cell-dependent intraepithelial MCs characterized in the jejunal mucosa during the height of a helminth infection preferentially express the chymases mMCP-1 and mMCP-2, but no elastase, neither of the tryptases nor CPA3. Only the mice lacking the cutaneous MC chymase mMCP-4 or the elastase mMCP-5 were significantly protected against the scald injury at the clinical and morphologic levels. Because an earlier report demonstrated that the mutation of *granzyme B* within the chymase locus on chromosome 14 disrupted the expression of other genes in the locus (42), we evaluated the injury in mice with a mutant *mMCP-1* gene, which is present in the same locus as the *mMCP-4* and *mMCP-5* genes (19). The lack of protection against scald burn in the mMCP-1–deficient mice indicates that only the respective mutations of *mMCP-4* and *mMCP-5* in the locus are each important.

mMCP-4 and mMCP-5 are highly homologous serine proteases that are encoded by different genes on mouse chromosome 14C1 that give them distinct substrate specificities. The mouse and rat chymases, mMCP-4 and rMCP-4, represent homologues of human MC chymase-1 on the basis of sequence homology and similarities in substrate specificity, including their ability to generate the angiotensin II fragment from angiotensin I (33, 43–45). The mouse and rat MC proteases, mMCP-5 and rMCP-5, each have a distinct elastase substrate specificity due to a change of glycine to valine at position 216 (20, 21, 46). Surprisingly, the MC-specific exopeptidase CPA3 is coordinately expressed with mMCP-5, and the expression of each depends on the presence of the other through an as yet undefined posttranscriptional mechanism (28, 29, 38). However, in the recently developed mutant with enzymatically inactive CPA3 protein, the expression of mMCP-5 is intact (28), and the normal level of burn injury in these mice indicates that the absence of CPA3 in the mMCP-5$^{-/-}$ mice does not account for their protection against the scald burn. We have also observed that mMCP-4 is poorly expressed in mMCP-5–deficient MCs as assessed by both measurement of enzymatic activity and immunoblots of serosal MC, and this secondary deficiency may contribute to the small size of the secretory granule by histochemical detection (7). That topical rmMCP-5 or human elastase but not human chymase restored scald burn injury to the mMCP-5–deficient strain indicates that the level of mMCP-4 in this strain is sufficient to satisfy the nonredundant requirement for mMCP-4. We found that mMCP-4–deficient MCs were selectively deficient in only that protease as originally reported (32) and reconstituted full burn injury with the homologous human MC chymase. Taken together, these data indicate that these two proteases act nonredundantly in the pathway leading to the inflammation, ulceration, and tissue remodeling of our scald burn model.

Even with histologic evidence of some scald-induced epidermal injury in the protected mMCP-4– and mMCP-5–deficient mice, it is likely that only a small fraction of the protease applied for 1 h postburn is absorbed into the tissue. Hence, it seems reasonable to suggest that this activity could be provided endogenously by the activation of MCs at the burn site in the first 2 h. That the absence of either mMCP-4 or mMCP-5 abrogates development of a second-degree burn despite some scald-induced epidermal injury argues for their early action in facilitating a second-degree burn, and this is nicely supported by exogenous protease-specific reconstitution within the first hour postscald. The role of these proteases could be in amplifying exposure of the tissue epitope for natural IgM, augmenting the required activation and function of the complement pathway or mediating paracrine activation of the MCs (47, 48). Furthermore, these proteases could have direct tissue effects such as activation of matrix metalloproteinases by either mMCP-4 (30) or mMCP-5 with concomitant inactivation of TIMP-1 (49).

Because neutrophils were absent in the hind limb IR injury of the mouse that is also dependent on MCs (9) and their mMCP-5 (7) and mMCP-4 proteases (T. Shi and M. Gurish, unpublished observations), we believe that the critical elastase function in both models is mediated by mMCP-5 and that neutrophil-derived elastase encoded on mouse chromosome 10 (50) does not provide a redundant function either in time or location. Further, that the mutation that created the elastolytic function also is retained in the rat chymase locus favors a biologic purpose for nonredundant

functions of the MC-specific proteases, mMCP-4 and mMCP-5. The recognition that natural IgM, complement, and two MC proteases can mediate injury as different as a second-degree scald burn of skin and IR necrosis of hind limb muscle suggests function of an innate triad in trauma-induced inflammatory processes. It may be that local permeability and cellular injury allow for the lectin pathway to activate complement with consequent MC degranulation (4, 51, 52), which targets a profound downstream process leading to termination of the ulcer with scarring but not contracture.

Acknowledgments

Y.K. works for Teijin Pharma Limited.

Disclosures

The authors have no financial conflicts of interest.

References

1. Horton, J. W., W. J. Mileski, D. J. White, and P. Lipsky. 1996. Monoclonal antibody to intercellular adhesion molecule-1 reduces cardiac contractile dysfunction after burn injury in rabbits. *J. Surg. Res.* 64: 49–56.
2. Nwariaku, F. E. M., W. J. M. Mileski, E. J. Lightfoot, Jr., P. J. B. Sikes, and P. E. M. Lipsky. 1995. Alterations in leukocyte adhesion molecule expression after burn injury. *J. Trauma* 39: 285–288.
3. Weiser, M. R., J. P. Williams, F. D. Moore, Jr., L. Kobzik, M. Ma, H. B. Hechtman, and M. C. Carroll. 1996. Reperfusion injury of ischemic skeletal muscle is mediated by natural antibody and complement. *J. Exp. Med.* 183: 2343–2348.
4. Chan, R. K., S. I. Ibrahim, K. Takahashi, E. Kwon, M. McCormack, A. Ezekowitz, M. C. Carroll, F. D. Moore, Jr., and W. G. Austen, Jr. 2006. The differing roles of the classical and mannose-binding lectin complement pathways in the events following skeletal muscle ischemia-reperfusion. *J. Immunol.* 177: 8080–8085.
5. Chan, R. K., N. Verna, J. Afnan, M. Zhang, S. Ibrahim, M. C. Carroll, and F. D. Moore, Jr. 2006. Attenuation of skeletal muscle reperfusion injury with intravenous 12 amino acid peptides that bind to pathogenic IgM. *Surgery* 139: 236–243.
6. Suber, F., M. C. Carroll, and F. D. Moore, Jr. 2007. Innate response to self-antigen significantly exacerbates burn wound depth. *Proc. Natl. Acad. Sci. USA* 104: 3973–3977.
7. Abonia, J. P., D. S. Friend, W. G. Austen, Jr., F. D. Moore, Jr., M. C. Carroll, R. Chan, J. Afnan, A. Humbles, C. Gerard, P. Knight, et al. 2005. Mast cell protease 5 mediates ischemia-reperfusion injury of mouse skeletal muscle. *J. Immunol.* 174: 7285–7291.
8. Mukundan, C., M. F. Gurish, K. F. Austen, H. B. Hechtman, and D. S. Friend. 2001. Mast cell mediation of muscle and pulmonary injury following hindlimb ischemia-reperfusion. *J. Histochem. Cytochem.* 49: 1055–1056.
9. Bortolotto, S. K., W. A. Morrison, X. Han, and A. Messina. 2004. Mast cells play a pivotal role in ischaemia reperfusion injury to skeletal muscles. *Lab. Invest.* 84: 1103–1111.
10. Stevens, R. L., and R. Adachi. 2007. Protease-proteoglycan complexes of mouse and human mast cells and importance of their beta-tryptase-heparin complexes in inflammation and innate immunity. *Immunol. Rev.* 217: 155–167.
11. Pejler, G., M. Abrink, M. Ringvall, and S. Wernersson. 2007. Mast cell proteases. *Adv. Immunol.* 95: 167–255.
12. Serafin, W. E., E. T. Dayton, P. M. Gravallese, K. F. Austen, and R. L. Stevens. 1987. Carboxypeptidase A in mouse mast cells. Identification, characterization, and use as a differentiation marker. *J. Immunol.* 139: 3771–3776.
13. Reynolds, D. S., R. L. Stevens, W. S. Lane, M. H. Carr, K. F. Austen, and W. E. Serafin. 1990. Different mouse mast cell populations express various combinations of at least six distinct mast cell serine proteases. *Proc. Natl. Acad. Sci. USA* 87: 3230–3234.
14. Reynolds, D. S., R. L. Stevens, D. S. Gurley, W. S. Lane, K. F. Austen, and W. E. Serafin. 1989. Isolation and molecular cloning of mast cell carboxypeptidase A. A novel member of the carboxypeptidase gene family. *J. Biol. Chem.* 264: 20094–20099.
15. Weidner, N., and K. F. Austen. 1993. Heterogeneity of mast cells at multiple body sites. Fluorescent determination of avidin binding and immunofluorescent determination of chymase, tryptase, and carboxypeptidase content. *Pathol. Res. Pract.* 189: 156–162.
16. Irani, A. M., S. S. Craig, G. DeBlois, C. O. Elson, N. M. Schechter, and L. B. Schwartz. 1987. Deficiency of the tryptase-positive, chymase-negative mast cell type in gastrointestinal mucosa of patients with defective T lymphocyte function. *J. Immunol.* 138: 4381–4386.
17. Kaartinen, M., A. Penttilä, and P. T. Kovanen. 1994. Mast cells of two types differing in neutral protease composition in the human aortic intima. Demonstration of tryptase- and tryptase/chymase-containing mast cells in normal intimas, fatty streaks, and the shoulder region of atheromas. *Arterioscler. Thromb.* 14: 966–972.
18. McNeil, H. P., K. F. Austen, L. L. Somerville, M. F. Gurish, and R. L. Stevens. 1991. Molecular cloning of the mouse mast cell protease-5 gene. A novel secretory granule protease expressed early in the differentiation of serosal mast cells. *J. Biol. Chem.* 266: 20316–20322.
19. Gurish, M. F., J. H. Nadeau, K. R. Johnson, H. P. McNeil, K. M. Grattan, K. F. Austen, and R. L. Stevens. 1993. A closely linked complex of mouse mast cell-specific chymase genes on chromosome 14. *J. Biol. Chem.* 268: 11372–11379.
20. Kunori, Y., M. Koizumi, T. Masegi, H. Kasai, H. Kawabata, Y. Yamazaki, and A. Fukamizu. 2002. Rodent alpha-chymases are elastase-like proteases. *Eur. J. Biochem.* 269: 5921–5930.
21. Karlson, U., G. Pejler, B. Tomasini-Johansson, and L. Hellman. 2003. Extended substrate specificity of rat mast cell protease 5, a rodent alpha-chymase with elastase-like primary specificity. *J. Biol. Chem.* 278: 39625–39631.
22. Solivan, S., T. Selwood, Z. M. Wang, and N. M. Schechter. 2002. Evidence for diversity of substrate specificity among members of the chymase family of serine proteases. *FEBS Lett.* 512: 133–138.
23. Knight, P. A., S. H. Wright, C. E. Lawrence, Y. Y. Paterson, and H. R. Miller. 2000. Delayed expulsion of the nematode Trichinella spiralis in mice lacking the mucosal mast cell-specific granule chymase, mouse mast cell protease-1. *J. Exp. Med.* 192: 1849–1856.
24. Thakurdas, S. M., E. Melicoff, L. Sansores-Garcia, D. C. Moreira, Y. Petrova, R. L. Stevens, and R. Adachi. 2007. The mast cell-restricted tryptase mMCP-6 has a critical immunoprotective role in bacterial infections. *J. Biol. Chem.* 282: 20809–20815.
25. Shin, K., G. F. Watts, H. C. Oettgen, D. S. Friend, A. D. Pemberton, M. F. Gurish, and D. M. Lee. 2008. Mouse mast cell tryptase mMCP-6 is a critical link between adaptive and innate immunity in the chronic phase of Trichinella spiralis infection. *J. Immunol.* 180: 4885–4891.
26. Shin, K., P. A. Nigrovic, J. Crish, E. Boilard, H. P. McNeil, K. S. Larabee, R. Adachi, M. F. Gurish, R. Gobezie, R. L. Stevens, and D. M. Lee. 2009. Mast cells contribute to autoimmune inflammatory arthritis via their tryptase/heparin complexes. *J. Immunol.* 182: 647–656.
27. McNeil, H. P., K. Shin, I. K. Campbell, I. P. Wicks, R. Adachi, D. M. Lee, and R. L. Stevens. 2008. The mouse mast cell-restricted tetramer-forming tryptases mouse mast cell protease 6 and mouse mast cell protease 7 are critical mediators in inflammatory arthritis. *Arthritis Rheum.* 58: 2338–2346.
28. Schneider, L. A., S. M. Schlenner, T. B. Feyerabend, M. Wunderlin, and H. R. Rodewald. 2007. Molecular mechanism of mast cell mediated innate defense against endothelin and snake venom sarafotoxin. *J. Exp. Med.* 204: 2629–2639.
29. Stevens, R. L., D. Qui, H. P. McNeil, D. Friend, J. Hunt, K. F. Austen, and M. Zhang. 1996. Transgenic mice that possess a disrupted mast cell protease 5 (mMCP-5) gene cannot store carboxypeptidase A in their granules. *FASEB J.* 10: 1307 (Abstr.).
30. Tchougounova, E., A. Lundequist, I. Fajardo, J. O. Winberg, M. Abrink, and G. Pejler. 2005. A key role for mast cell chymase in the activation of pro-matrix metalloprotease-9 and pro-matrix metalloprotease-2. *J. Biol. Chem.* 280: 9291–9296.
31. McNeil, H. P., D. P. Frenkel, K. F. Austen, D. S. Friend, and R. L. Stevens. 1992. Translation and granule localization of mouse mast cell protease-5. Immunodetection with specific antipeptide Ig. *J. Immunol.* 149: 2466–2472.
32. Tchougounova, E., G. Pejler, and M. Abrink. 2003. The chymase, mouse mast cell protease 4, constitutes the major chymotrypsin-like activity in peritoneum and ear tissue. A role for mouse mast cell protease 4 in thrombin regulation and fibronectin turnover. *J. Exp. Med.* 198: 423–431.
33. Karlson, U., G. Pejler, G. Froman, and L. Hellman. 2002. Rat mast cell protease 4 is a beta-chymase with unusually stringent substrate recognition profile. *J. Biol. Chem.* 277: 18579–18585.
34. Hallgren, J., U. Karlson, M. Poorafshar, L. Hellman, and G. Pejler. 2000. Mechanism for activation of mouse mast cell tryptase: dependence on heparin and acidic pH for formation of active tetramers of mouse mast cell protease 6. *Biochemistry* 39: 13068–13077.
35. Henningsson, F., P. Wolters, H. A. Chapman, G. H. Caughey, and G. Pejler. 2003. Mast cell cathepsins C and S control levels of carboxypeptidase A and the chymase, mouse mast cell protease 5. *Biol. Chem.* 384: 1527–1531.
36. Hunt, J., and R. L. Stevens. 1995. Mouse mast cell proteases. In *Biological and Molecular Aspects of Mast Cell and Basophil Differentiation and Function.* S. J. Galli, Y. Kitamura, S. Yamamoto, and M. Greaves, eds. Raven Press, New York, p. 149–160.
37. Hunt, J. E., R. L. Stevens, K. F. Austen, J. Zhang, Z. Xia, and N. Ghildyal. 1996. Natural disruption of the mouse mast cell protease 7 gene in the C57BL/6 mouse. *J. Biol. Chem.* 271: 2851–2855.
38. Feyerabend, T. B., H. Hausser, A. Tietz, C. Blum, L. Hellman, A. H. Straus, H. K. Takahashi, E. S. Morgan, A. M. Dvorak, H. J. Fehling, and H. R. Rodewald. 2005. Loss of histochemical identity in mast cells lacking carboxypeptidase A. *Mol. Cell. Biol.* 25: 6199–6210.
39. Kitamura, Y., S. Go, and K. Hatanaka. 1978. Decrease of mast cells in W/Wv mice and their increase by bone marrow transplantation. *Blood* 52: 447–452.
40. Chervenick, P. A., and D. R. Boggs. 1969. Decreased neutrophils and megakaryocytes in anemic mice of genotype W/W. *J. Cell. Physiol.* 73: 25–30.
41. Zhou, J. S., W. Xing, D. S. Friend, K. F. Austen, and H. R. Katz. 2007. Mast cell deficiency in Kit(W-sh) mice does not impair antibody-mediated arthritis. *J. Exp. Med.* 204: 2797–2802.
42. Pham, C. T., D. M. MacIvor, B. A. Hug, J. W. Heusel, and T. J. Ley. 1996. Long-range disruption of gene expression by a selectable marker cassette. *Proc. Natl. Acad. Sci. USA* 93: 13090–13095.

43. Kunori, Y., Y. Muroga, M. Iidaka, H. Mitsuhashi, T. Kamimura, and A. Fukamizu. 2005. Species differences in angiotensin II generation and degradation by mast cell chymases. *J. Recept. Signal Transduct. Res.* 25: 35–44.
44. Caughey, G. H., W. W. Raymond, and P. J. Wolters. 2000. Angiotensin II generation by mast cell alpha- and beta-chymases. *Biochim. Biophys. Acta* 1480: 245–257.
45. Andersson, M. K., U. Karlson, and L. Hellman. 2008. The extended cleavage specificity of the rodent beta-chymases rMCP-1 and mMCP-4 reveal major functional similarities to the human mast cell chymase. *Mol. Immunol.* 45: 766–775.
46. Huang, R. Y., T. Blom, and L. Hellman. 1991. Cloning and structural analysis of MMCP-1, MMCP-4 and MMCP-5, three mouse mast cell-specific serine proteases. *Eur. J. Immunol.* 21: 1611–1621.
47. Schwartz, L. B., M. S. Kawahara, T. E. Hugli, D. Vik, D. T. Fearon, and K. F. Austen. 1983. Generation of C3a anaphylatoxin from human C3 by human mast cell tryptase. *J. Immunol.* 130: 1891–1895.
48. Schick, B., K. F. Austen, and L. B. Schwartz. 1984. Activation of rat serosal mast cells by chymase, an endogenous secretory granule protease. *J. Immunol.* 132: 2571–2577.
49. Jackson, P. L., X. Xu, L. Wilson, N. M. Weathington, J. P. Clancy, J. E. Blalock, and A. Gaggar. 2010. Human neutrophil elastase-mediated cleavage sites of MMP-9 and TIMP-1: implications to cystic fibrosis proteolytic dysfunction. *Mol. Med.* 16: 159–166.
50. Belaaouaj, A., B. C. Walsh, N. A. Jenkins, N. G. Copeland, and S. D. Shapiro. 1997. Characterization of the mouse neutrophil elastase gene and localization to chromosome 10. *Mamm. Genome* 8: 5–8.
51. el-Lati, S. G., C. A. Dahinden, and M. K. Church. 1994. Complement peptides C3a- and C5a-induced mediator release from dissociated human skin mast cells. *J. Invest. Dermatol.* 102: 803–806.
52. Kimura, T., A. Andoh, Y. Fujiyama, T. Saotome, and T. Bamba. 1998. A blockade of complement activation prevents rapid intestinal ischaemia-reperfusion injury by modulating mucosal mast cell degranulation in rats. *Clin. Exp. Immunol.* 111: 484–490.